Plant, Cell & Environment

Plant, Cell and Environment (2013) **36**, 2190–2206 doi: 10.1111/pce.12129

Original Article

Isotopic composition of transpiration and rates of change in leaf water isotopologue storage in response to environmental variables

KEVIN A. SIMONIN[1]*†, ADAM B. RODDY[2†], PERCY LINK[3], RANDY APODACA[4], KEVIN P. TU[2,‡], JIA HU[1], TODD E. DAWSON[2] & MARGARET M. BARBOUR[1]

[1]*Faculty of Agriculture and Environment, University of Sydney, Sydney, NSW 2570, Australia,* [2]*Department of Integrative Biology, University of California-Berkeley, Berkeley, CA 94720, USA,* [3]*Department of Earth and Planetary Science, University of California-Berkeley, Berkeley, CA 94720, USA and* [4]*Department of Chemistry, University of California-Berkeley, Berkeley, CA 94720, USA*

ABSTRACT

During daylight hours, the isotope composition of leaf water generally approximates steady-state leaf water isotope enrichment model predictions. However, until very recently there was little direct confirmation that isotopic steady-state (ISS) transpiration in fact exists. Using isotope ratio infrared spectroscopy (IRIS) and leaf gas exchange systems we evaluated the isotope composition of transpiration and the rate of change in leaf water isotopologue storage (isostorage) when leaves were exposed to variable environments. In doing so, we developed a method for controlling the absolute humidity entering the gas exchange cuvette for a wide range of concentrations without changing the isotope composition of water vapour. The measurement system allowed estimation of ^{18}O enrichment both at the evaporation site and for bulk leaf water, in the steady state and the non-steady state. We show that non–steady-state effects dominate the transpiration isoflux even when leaves are at physiological steady state. Our results suggest that a variable environment likely prevents ISS transpiration from being achieved and that this effect may be exacerbated by lengthy leaf water turnover times due to high leaf water contents.

Key-words: stable water isotopes; steady state; transpiration.

INTRODUCTION

Variation in the oxygen-stable isotope ratios ($\delta^{18}O$) of ecosystem water pools can reveal important information about water flux pathways that define local, regional, and global water and carbon cycling (Farquhar *et al*. 1993; Gat 1996; Ciais *et al*. 1997; Yakir & Sternberg 2000). Until relatively recently one major methodological limitation to using $\delta^{18}O$ in ecosystem–atmosphere water and carbon exchange models was our inability to measure the $\delta^{18}O$ of water, in the liquid and vapour phases, and atmospheric CO_2 at high temporal frequencies. With the advent of optically based technologies this limitation has largely been overcome (e.g. Griffis *et al*. 2005; Barbour *et al*. 2007; Helliker & Noone 2010; Wingate *et al*. 2010). However further complications may exist when defining the isotope model parameters used to differentiate between the terrestrial flux pathways that ultimately contribute to variation in the $\delta^{18}O$ of atmospheric water vapour and CO_2. For example, isoflux models used to evaluate the influence of vegetation on water and carbon cycling often assume that transpiration occurs at isotopic steady state (ISS; Flanagan, Comstock & Ehleringer 1991; Farquhar & Lloyd 1993). Because the uptake and transport of water from soil to the evaporation site in leaves of most plants occurs without isotope fractionation, at ISS, the $\delta^{18}O$ of transpiration ($\delta^{18}O_{trans}$) is operationally defined as being equal to plant–stem xylem water ($\delta^{18}O_S$). However direct measurements of $\delta^{18}O_{trans}$ are relatively rare, and the few direct measurements of $\delta^{18}O_{trans}$ that exist suggest that $\delta^{18}O_{trans}$ is often not equal to $\delta^{18}O_S$ (Yakir *et al*. 1994; Wang & Yakir 1995; Harwood *et al*. 1998, 1999; Wang *et al*. 2011). Yet, during daytime hours, the isotope composition of leaf water is often well characterized by steady-state leaf water-enrichment models (Cernusak, Pate & Farquhar 2002; Kahmen *et al*. 2008). Therefore in order to accurately parameterize ecosystem–atmosphere water and carbon exchange models, a better understanding of the processes regulating isotopic steady-state versus non–steady-state transpiration is needed.

Theory

As described by Farquhar & Cernusak (2005), the flux of the heavy isotopes of water through leaves to the atmosphere and the rate of change in the amount of heavy leaf water enrichment are linked as:

$$\frac{d(W \cdot R_L)}{dt} = R_S J - R_{trans} E \quad (1)$$

where R_L, R_S and R_{trans} are the heavy to light isotope ratios (e.g. $^{18}O/^{16}O$) of leaf water, source water and the evaporating water; W is leaf water content (mol m^{-2}); J is the flux of water

Correspondence: K. A. Simonin. Tel: +61 02 9351 8882; e-mail: kevin.simonin@sydney.edu.au

†These authors contributed equally to this work.
‡Current affiliation: Pioneer Hi-Bred International, Woodland, CA 95695, USA.

to the evaporation sites in the leaf (mol $m^{-2} s^{-1}$); and E is the evaporation flux (mol $m^{-2} s^{-1}$). Expressing leaf water and the evaporation flux as enrichments above source water, Eqn 1 can be rewritten as (Farquhar & Cernusak 2005):

$$\frac{d(W \cdot \Delta_L)}{dt} = -E\Delta_{trans} \quad (2)$$

where $\Delta_L = R_L/R_S - 1$, and $\Delta_{trans} = R_{trans}/R_S - 1$. According to Eqn 2, if $R_{trans} = R_S$, then Δ_{trans} is zero, the rate of change in the storage of leaf water isotopologues (termed here, 'isostorage'; left side of Eqn 2) is zero, and Δ_{trans} and Δ_L are considered to be at ISS. In the present study, we are interested in the biological and environmental factors that influence variation in Δ_{trans} and Δ_L, and thus the conditions that may cause R_{trans} to deviate from R_S leading to non–steady-state transpiration.

According to stable isotope theory, fractionation during evaporation is a two-phase process that involves: (1) a liquid–vapour equilibrium isotope effect as influenced by temperature-dependent differences in the saturation vapour pressures of the heavy and light water isotopologues and (2) kinetic isotope effects that occur as water vapour is transported away from the air–water interface. This two-phase process was firstly described by Craig & Gordon (1965) for evaporation from well-mixed surface waters and subsequently applied to transpiration as (Dongmann *et al*. 1974; Farris & Strain 1978; Farquhar *et al*. 1989; Flanagan *et al*. 1991; Farquhar & Lloyd 1993; Harwood *et al*. 1998; Farquhar & Cernusak 2005):

$$R_{trans} = \frac{R_e - \alpha^+ R_v \frac{w_a}{w_i}}{\alpha^+ \alpha_k \left(1 - \frac{w_a}{w_i}\right)} \quad (3)$$

where R_e and R_V are the heavy to light isotope ratios of liquid water at the evaporation site and water vapour outside the leaf, w_i and w_a are the mole fractions (mol mol^{-1}) of water vapour inside the leaf and in the ambient atmosphere, $\alpha+$ is the temperature-dependent equilibrium isotope fractionation factor (Majoube 1971) and α_k is the kinetic fractionation factor (Merllivat 1978; Farquhar *et al*. 1989; Barkan & Luz 2007). The kinetic fractionation factor describing the ratio of the diffusion coefficients of the heavy and light water isotopologues as water vapour passes through the leaf stomata and boundary layer in series is defined as:

$$(\alpha_k - 1) = \frac{28r_s + 19r_b}{r_s + r_b} \Big/ 1000 \quad (4)$$

where r_s and r_b are stomata and boundary layer resistances, (Merllivat 1978; Farquhar *et al*. 1989; Barkan & Luz 2007). According to Eqns 3 and 4, R_{trans} and, by extension, the rate of change in leaf isostorage (i.e. $\frac{d(W \cdot R_L)}{dt}$ from Eqn 1), are sensitive to variation in leaf temperature by way of changes in $\alpha+$ and w_i, to variation in leaf surface conductance (i.e. r_s and r_b) by way of changes in α_k and transpiration induced changes in leaf temperature, and to ambient humidity (i.e. w_a). Eqn 3 can be converted to delta notation as (Yakir & Sternberg 2000):

$$\delta_{trans} = \frac{\alpha_{eq}\delta_e - \frac{w_a}{w_i}\delta_v - \varepsilon^+ - \left(1 - \frac{w_a}{w_i}\right)\varepsilon_k}{\left(1 - \frac{w_a}{w_i}\right) + \left(1 - \frac{w_a}{w_i}\right)\varepsilon_k} \quad (5)$$

where $\varepsilon^+ = \alpha^+ - 1$ and $\varepsilon_k = \alpha_k - 1$.

The utility of Eqns 3 or 5 for characterizing the isotope composition of transpiration in response to a variable environment is quite limited because of the difficulties of directly quantifying the isotope composition of water at the evaporation site. However, given enough time at constant w_a, w_i, R_S, R_V, α_k and $\alpha+$, R_{trans} should approach R_S, leading to ISS, and at ISS the rate of change in leaf isostorage (left side of Eqn 2) is expected to approach zero (Dongmann *et al*. 1974). Therefore, the steady-state assumption that $R_{trans} \approx R_S$ allows Eqn 3 to be used to evaluate changes in the isotope compositions of liquid water at the evaporation site in response to a variable environment (Farquhar *et al*. 1989; Flanagan *et al*. 1991). Replacing R_{trans} with R_S in Eqn 3 and rearranging the equation, the steady-state isotope composition of liquid water at the evaporation site (R_{es}) can be modeled as:

$$R_{es} = \alpha^+ \left[\alpha_k R_S \left(1 - \frac{w_a}{w_i}\right) + R_V \frac{w_a}{w_i}\right] \quad (6)$$

or as enrichment above source water (Δ_{es}):

$$\Delta_{es} = \varepsilon^+ + \varepsilon_k + (\Delta_V - \varepsilon_k)\frac{w_a}{w_i} \quad (7)$$

Many empirical studies have found that bulk leaf water is often less enriched in the heavy water isotopologues than liquid water at the evaporation site based on Eqn 7 (e.g. Allison, Gat & Leaney 1985; Bariac *et al*. 1989; Yakir, DeNiro & Rundel 1989; Walker & Brunel 1990; Flanagan *et al*. 1991, 1994; Wang, Yakir & Avishai 1998). Two main hypotheses were proposed to explain this discrepancy. The first hypothesis proposed that hydraulic compartmentalization in the leaf would preclude complete mixing of enriched and unenriched parts of the bulk leaf water (White 1983). Although there was evidence for the existence of more than one leaf water pool (Yakir *et al*. 1989; Yakir, DeNiro & Gat 1990), critics argued that this hypothesis could not explain why the discrepancy between Δ_L and Δ_{es} seen in many empirical studies seemed to covary with transpiration rate (Walker *et al*. 1989; Flanagan *et al*. 1991, 1994). The dependence on transpiration rate of the difference between modeled Δ_e and empirical measurements of Δ_L led to widespread support for the second hypothesis, which explained this discrepancy as arising from gradients of isotopes within the leaf (Farquhar & Lloyd 1993; Barbour *et al*. 2000). Because water is enriched at the evaporation site, diffusion favours the flow of enriched water in the opposite direction of the convection of unenriched water in the transpiration stream, a process referred to as the Péclet effect. Because the second hypothesis provided a mechanism to explain why the discrepancy between measured Δ_L and modeled Δ_e varied with transpiration rate, the first hypothesis has largely been ignored ever since.

Incorporating the Péclet effect into Eqn 7, the average steady-state bulk leaf water enrichment (i.e. Δ_{LS}) can be modeled as:

$$\Delta_{LS} = \frac{\Delta_{es}(1-e^{-\wp})}{\wp} \quad (8)$$

where $\wp$ is the Péclet term, a dimensionless number that takes into account the incomplete mixing of leaf water because of the mass flow of water from the xylem opposing the back-diffusion of enriched water (Farquhar & Lloyd 1993). The Péclet number is defined as EL/CD, where L is the effective path length for water transport from the xylem to the evaporation site (m); C is the molar concentration of water (mol m^{-3}); and D is the diffusivity (m^2 s^{-1}).

Although daytime variation in Δ_L is often well characterized by steady-state model predictions that incorporate Péclet effects (Cernusak *et al*. 2002; Kahmen *et al*. 2008), transpired water (R_{trans}) can nonetheless deviate from source water (R_S) when exposed to short-term fluctuations in the environment (Yakir *et al*. 1994; Wang & Yakir 1995; Harwood *et al*. 1998, 1999; Wang *et al*. 2011). How much R_{trans} deviates from R_S and for how long remains unclear, largely because of limited available data. However, some reports show that $\delta^{18}O$ of transpired water may deviate from source water by as much as 18‰ (Harwood *et al*. 1998) to 100‰ (Welp *et al*. 2008) under naturally varying conditions. Only recently have we been able to measure the transpiration isoflux with higher temporal resolution.

Simultaneous measurement of leaf gas exchange and the isotope composition of transpired water allows calculation of isotope enrichment at the evaporation site in the non-steady state (Δ_e, where $\Delta_e = R_e/R_s - 1$) by replacing R_S in Eqn 6 with R_{trans} (Harwood *et al*. 1998);

$$R_e = \alpha^+\left[\alpha_k R_{trans}\left(1-\frac{w_a}{w_i}\right)+R_v\left(\frac{w_a}{w_i}\right)\right] \quad (9)$$

Further, using measurements of transpiration rate (E) and enrichment of transpired water (Δ_{trans}) combined with leaf water content (W, and assuming W is constant in the first instance) to parameterize Eqn 2, we can calculate the enrichment of bulk leaf water (Δ_L), and therefore the Peclét effective length (L) from Eqn 8. This assumes that Eqn 8 can be used in the non-steady state when R_{trans} is not equal to R_s (Farquhar & Cernusak 2005). Using the new Δ_{trans} measurement techniques described here and existing theoretical models we are able to reassess the original steady-state transpiration assumption and, by extension, how the ISS assumption impacts the Péclet component of leaf water enrichment models, in particular the effective path length (L).

Here we evaluate the $\delta^{18}O$ of transpiration in response to changes in w_a/w_i, $\delta^{18}O_V$, ε_k, and $\varepsilon+$ and, as a result, the frequency (or infrequency) of ISS transpiration and the rate of change in leaf isostorage (i.e. $\frac{d(W\cdot\Delta_L)}{dt}$). Our study had five goals. Firstly, we wanted to develop a new method to measure the heavy to light isotope composition of transpiration and the leaf water isoflux (i.e. $R_{trans}E$) that relies on isotope ratio infrared spectroscopy (IRIS) and highlight how an IRIS instrument can be coupled to leaf gas exchange systems. In doing so, we also developed and implemented a method for controlling the absolute humidity entering the leaf gas exchange cuvette for a wide range of water vapour concentrations (approximately 4000–22000 ppmv) while maintaining a constant $\delta^{18}O$ of water vapour entering the cuvette. Secondly, we quantified variation in the isotope composition of transpired water vapour, the leaf water isoflux and the rate of change in leaf isostorage that can occur as a result of (1) changes in the isotope ratios of water vapour entering the cuvette (i.e. shifts in R_V); and (2) changes in leaf surface conductance to water vapour. Thirdly, we examined the differences between steady-state and non–steady-state model predictions of leaf water enrichment at the evaporation site. Fourthly, we evaluated how much steady-state and non–steady-state model predictions of the effective path length, L, may differ. Fifthly, we performed a sensitivity analysis of the transpiration isotope model (i.e. Eqns 3 & 5) to variation in g_s, T_L and w_a/w_i and compared the results of the model sensitivity analysis to our empirical observations.

MATERIALS AND METHODS

Plant growth conditions

We evaluated the isotope composition of transpiration from leaves of tobacco (*Nicotiana tabacum*, genotype WT38) and *Citrus* spp. Tobacco plants were grown in 5 L pots with potting mix (amended with Osmocote, Scotts, Australia) at the University of Sydney in a controlled environment growth cabinet set at 30/20 °C day/night temperature, 75% relative humidity and approximately 700 μmol m^{-2} s^{-1} PPFD (photosynthetic photon flux density) at the level of the upper leaves. Growth CO_2 concentration was not controlled, but varied from 370 to 420 ppm during the light period of 14 h. Plants were well-watered throughout their growth. *Citrus* spp. were grown in 5 L pots using commercial potting soil (Supersoil Potting Soil; Supersoil and Rod McLellan, Marysville, OH, USA). Plants were exposed to normal variation in sunlight, temperature and humidity, and were well-watered throughout their growth.

Vapourization module for humidifying dry air

In both gas exchange systems, air was humidified without isotopic fractionation by a custom-built vapourization module, similar to commercially available instruments (Los Gatos Research, Mountain View, CA, USA). The vapourization module had two inputs for supply gases, each controlled by a mass flow controller. The 'wet' mass flow controller directed flow to a 25 μL C-flow nebulizer (C-flow Nebulizer; part # 950-800-1380; Savillex Corporation, Minnetonka, MN, USA) that relied on capillary action to draw water from a reservoir. This water was vapourized by the air from the 'wet' controller into a 150 mL chamber (Savillex Corporation) heated to 130 °C, ensuring complete vapourization without fractionation of the incoming water. Air from the

'dry' controller was injected directly into this heated chamber, so that vapour concentrations were controlled by adjustments in flow rates both to the nebulizer and to the heated, diluting chamber. The humidified air then flowed from the heated chamber via tubing to the gas exchange systems described later. All components of the vapourization module were made from perfluoroalkoxy (PFA).

MPH-1000 gas exchange and water vapour isotope measurement system

Gas exchange measurements and cuvette conditions were controlled by an MPH-1000 Plant Gas Exchange System (Campbell Scientific Inc., Logan, UT, USA). In this system, water vapour concentrations were measured by chilled mirror hygrometers (DEW-10, General Eastern, Billerica, MA, USA), and CO_2 concentrations were measured by an LI-6252 infrared gas analyser in differential mode (LiCor Biosciences, Lincoln, NE, USA). Cuvette air was mixed from separate tanks of N_2, CO_2 and O_2, the concentrations of which were regulated by mass flow controllers in the gas exchange system. A fine-wire thermocouple was located inside the chamber and was positioned to touch the center of the abaxial side of the leaf. Individual components of the gas exchange system were interfaced to a CR10 datalogger (Campbell Scientific Inc., Logan, UT, USA), which calculated fluxes, controlled cuvette conditions and recorded data every 5 s. Projected leaf area in the chamber was measured from digital images of the leaf, using imaging software (ImageJ, US NIH, Bethesda, MD, USA), and all fluxes were corrected to the one-sided leaf area in the cuvette.

We modified the gas exchange system so that absolute humidity supplied to the cuvette could vary while maintaining a constant isotope composition. In this modification, air supplied from the N_2 and O_2 tanks was mixed and split between two mass flow controllers, which flowed to the 'wet' and 'dry' paths described earlier. After the vapourization chamber, this humidified air was then returned to the gas exchange system and mixed with CO_2. Approximately 800 mL min^{-1} of the total flow was split to the reference line, where it passed through a flow regulator and then was measured for water vapour and CO_2 concentrations. The other 800 mL min^{-1} of flow continued to a mass flow meter and then to the stainless steel cuvette. Junctions for sampling by the IRIS instrument were placed immediately before and after the cuvette. We alternated sampling for water vapour isotope ratios before and after the cuvette for 4 min at each location. The IRIS instrument drew approximately 30 mL min^{-1}. After exiting the cuvette, the remaining flow continued on to a flow regulator, passed through a pump, then through a chilled mirror hygrometer, and finally to the LI-6252, which measured CO_2 concentration. Because of pressure dependence in the LI-6252, the two flow regulators were constantly and manually adjusted to balance their flows to the infrared gas analyzer (IRGA). All tubing before the vapourization module was Bev-a-Line IV (Thermoplastic Processes, Stirling, NJ, USA) and all tubing after the vapourization module was PFA. In previous tests, Bev-a-Line IV did not cause any measurable fractionation (Apodaca and Simonin, unpublished data), although PFA may have fewer memory effects (Schmidt *et al*. 2010). During all measurements, we maintained cuvette dewpoint temperature at least 5 °C above ambient room temperature to ensure that no condensation occurred in the cuvette or tubing. A diagram of this setup is presented in Supporting Information Figure S1.

LI-6400 gas exchange and water vapour isotope measurement system

Two LI-6400 portable photosynthesis systems (Li6400xt, LiCor Inc., Lincoln, NE, USA) were modified to use humidified air supplied by the vapourization module described earlier. For this system, CO_2-free dry air was supplied to the vapourization module by splitting flow to two mass flow controllers. The vapour concentration produced by the vapourization module was regulated by manually controlling flow rates through the 'wet' and 'dry' mass flow controllers. The humidified air exited the vapourization module through PFA tubing, from which (1) a subsample was plumbed to the IRIS instrument through a normally closed valve and (2) the two Li6400xt systems drew their supply gas. Flow rates from the vapourization module exceeded the combined flow rates into the two Li6400xt systems and the IRIS, and the excess flow produced by the vapourization module flowed through a long length of PFA tubing placed after the point where the two Li6400xt and the IRIS drew their supply gas to prevent isotopic backflow and contamination of the gas supplied to the instruments. In both Li6400xt systems, the soda lime and desiccant columns were bypassed, and CO_2 was added using the internal CO_2 mixer. Internal tubing in the Li6400xt was Bev-a-Line IV. The standard 2×3 cm chamber with a blue–red light source was used on both LI-6400 s. A manual three-way valve was placed in the leaf chamber exit tube to allow alternate sampling by the IRIS instrument and matching the IRGAs. IRGAs were matched at least every 30 min. When not in match mode, the exit air stream from each leaf chamber was directed to normally closed valves connected with short lengths of tubing to the IRIS instrument. Long lengths of PFA tubing were connected just upstream of the valves to allow the excess air flow from the leaf chamber to go to waste without backflow. The air stream from the vapourization module (leaf chamber inlet) and the two leaf chamber outlet air streams were sampled sequentially, controlled by the IRIS valve sequencer software. A diagram of this setup is presented in Supporting Information Figure S2.

Isotope measurements

Both systems used water vapour isotope analyzers (L1102-i) from Picarro Inc. (Sunnyvale, CA, USA), which calculate the $\delta^{18}O$ of water vapour from spectral absorbance in specific wavelengths. All measurements are expressed in per mil (‰) as:

$$\delta^{18}O = \left(\frac{R_{sample}}{R_{standard}} - 1 \right) \quad (10)$$

where R is the ratio of the heavy to light isotope ($^{18}O/^{16}O$) of the sample (R_{sample}) and of the V-SMOW standard ($R_{standard}$). Two calibration standards bracketing the range of measured values were used to calibrate each instrument. These measurements of $\delta^{18}O$ showed a concentration dependence that was instrument-specific. We characterized the dependence of $\delta^{18}O$ measurements on the concentration of water vapour for both IRIS instruments across a wide range of concentrations (approximately every 2000–4000 ppmv spanning from 3000 to 25 000 ppmv) and isotope ratios before any gas exchange measurements were made. Additionally at the end of each day of gas exchange measurements, we introduced standards spanning the range of measured isotope ratios and concentrations. To correct for concentration dependencies, we firstly linearly regressed the actual isotope ratios (determined by traditional isotope ratio mass spectrometry; see later) against the measured isotope ratios at a fixed concentration of 10 000–10 200 ppmv, and then we applied this linear model to all measurements. We then plotted the residual isotope error (actual minus partially corrected measured) against water vapour concentration, and fit a polynomial to this relationship for each isotope. We used these fitted equations (actual versus measured delta value, and residual delta error versus concentration) to correct all experimental measurements.

The IRIS instruments measure approximately every 6 s, but for our application, we used a manifold to switch between sampling before and after the cuvette. After each switch, we discarded measurements to allow for flushing of the previous sample through the optical cell and tubing and to allow for dissipation of transient pressure variation because of switching between sampling locations. For measurements made using the MPH-1000, the IRIS sampled for 4 min at each location, and the first minute of measurements were discarded. For measurements made using the Li6400xt, the IRIS sampled for 3 min at each location. The first 2.5 min were discarded and an average calculated from the last 30 s.

Because the air stream after the cuvette was a mixture of water vapour supplied to the cuvette and vapour transpired by the leaf, we calculated the isotope ratios of transpired water vapour as (Evans & von Caemmerer, personal communication):

$$\delta^{18}O_{trans} = \left(\delta^{18}O_{out}(1-w_{in}) - \delta^{18}O_{in}\frac{w_{in}}{w_{out}}(1-w_{out})\right)\frac{w_{out}}{(w_{out}-w_{in})} \quad (11)$$

where $\delta^{18}O_{in}$, w_{in} and $\delta^{18}O_{out}$, w_{out} are the isotope compositions and mole fractions of the water vapour entering and leaving the cuvette, respectively. We used the mole fractions before and after the cuvette measured by the gas exchange systems in this equation.

Isotope ratios of source water were determined by sampling the water used to irrigate the plants during the duration of the experiment or by sampling the petiole and stem subtending the leaf. Because the tobacco plants were kept well-watered, we assumed minimal evaporative enrichment in the soil such that the water applied to the plants was isotopically identical to soil source water. In this case, the vapourization module described earlier was used to measure irrigation water after calibration procedures were complete. Irrigation water was sampled daily, but varied only a little during the experiment ($\delta^{18}O = -3.4$ to -3.1‰). For the *Citrus* plants, we sampled the petiole and stem immediately subtending the measured leaf at the end of the day and extracted this water using cryogenic distillation. Isotope ratios of the plant extracted water and the working standards used with the MPH-1000 system were measured on a Thermo Finnigan MAT Delta plus XL mass spectrometer interfaced with the Gas Bench (for $\delta^{18}O$) and H/Device Cr-reduction system (for $\delta^{2}H$; Bremen, Germany) at the University of California, Berkeley. The long-term precision for these methods on this instrument is ±0.17‰ for $\delta^{18}O$. The working standards used with the LI-6400 system were measured on the Picarro against VSMOW, GISP and VSLAP2. The standard deviation of the results of the four independent analyses was ±0.11‰ for $\delta^{18}O$.

We calculated fractionation factors based on the gas exchange measurements. The equilibrium fractionation factor (ε^{+}) was calculated according to Majoube (1971).

The kinetic fractionation factor (ε_k) was calculated from stomatal ($g_s = 1/r_s$) and boundary layer ($g_b = 1/r_b$) conductances according to Eqn 4. Additionally, we calculated the residence time of leaf water as (Farquhar & Cernusak 2005):

$$\tau = \frac{W}{g w_i} \quad (12)$$

where τ is leaf water residence time (s); W is leaf water concentration (mol m^{-2}); g is total leaf conductance (stomata plus boundary layer conductance; mol $m^{-2}\,s^{-1}$); and w_i is the mole fraction of water vapour inside the leaf (mol mol^{-1}). Residence times were calculated based on the 5–20 min preceding each change in either c_a or vapour source. W was estimated based on measurements of five leaves per species, and the average value for each species was used in the calculations.

Experimental measurements

In all measurements made using the Li6400xt only a portion of a leaf was enclosed in the leaf chamber. When using the MPH-1000, the entire leaf lamina was fully enclosed in the leaf chamber. In both systems, the leaf chambers were leak-tested by breathing around the chamber gasket. While using the Li6400xt we varied the isotope ratio of water vapour entering the leaf chamber while maintaining relatively constant absolute humidity. Using both gas exchange systems, we varied the atmospheric CO_2 concentration (c_a) to induce changes in stomatal conductance (g_s).

Leaves of four WT38 tobacco plants were subjected to changes in the isotope ratio of the water vapour supplied to the leaf chamber. We changed the isotope ratios of vapour in two steps, with 74–120 min of measurements before the first change and during each background vapour source. The first background vapour had a $\delta^{18}O$ of –15.0‰. The second background vapour had a $\delta^{18}O$ of –1.1‰. This second background

vapour source was chosen to be isotopically heavier than transpired water so as to decouple the concentration and isotope differences driving the transpiration isoflux. A second step change returned the background vapour to the original source. In this experiment, block temperature of the Li6400xt was controlled at 30 °C, light at 2000 μmol m^{-2} s^{-1} and the CO_2 concentration within the leaf chamber at 500 μmol mol^{-1}.

On four different leaves from four WT38 tobacco plants we made a single step change in c_a from 400 to 800 ppm by controlling the CO_2 concentration of air within the leaf chamber (Li6400xt). For these leaves, measurements were made approximately 40 min before and after the change in c_a. Gas exchange was measured continuously and logged every minute. The block temperatures of the Li6400xt were controlled at 30 °C, and the light level at 2000 μmol m^{-2} s^{-1}. Flow rate through the leaf chamber was 300 μmol s^{-1}.

In three *Citrus* leaves (MPH-1000), we varied c_a across a wide range of concentrations from 100–900 ppm to induce changes in g_s, although for clarity here we report only two of these changes (400–730 and 730–900). Gas exchange measurements using this system were logged every 5 s and plotted as 1-min averages. Isotope measurements were made for approximately 24 min at each CO_2 concentration, alternating isotope sampling before and after the cuvette.

Data analysis

In the first part of our analysis we use the leaf water isostorage model (Eqns 1 & 2) described by Farquhar & Cernusak (2005) to model the influence of leaf water content (W) on leaf water enrichment (Δ_L). We calculated the rate of change in leaf isostorage ($-E\Delta_{trans}$) and solved for Δ_L in Eqn 2 from direct measurements of E, R_{trans} and R_S along with measured and simulated values of W. In this analysis we assumed W was constant over the time period during which $-E\Delta_{trans}$ was calculated. This is probably unrealistic when transpiration rate changes dramatically, and we will explore this situation in a subsequent paper. Additionally, we used measured values of R_{trans} and R_S to evaluate differences between steady-state and non–steady-state calculations of water enrichment at the evaporation site (Δ_{es} and Δ_e using Eqns 6 & 9).

In the second part of our analysis we evaluated the differences between steady-state and non–steady-state model predictions of the effective path length (L_S and L_{NS}, respectively). In this analysis we forward modeled leaf water enrichment from different Δ_L 'starting points' using Eqn 2 and direct measurements of W, E and Δ_{trans}, as described earlier. We then used our estimates of R_S and Eqns 6 and 7 to model Δ_{es} and determined L_S at each time point iteratively using the best fit of Eqn 8. The same procedure was used for determining L_{NS} using Eqns 8 and 9 assuming that Eqn 8 is valid in the non-steady state (Farquhar & Cernusak 2005). Additionally we compared the sensitivity of $\delta^{18}O_{trans}$ to variation in w_a/w_i, T_L, g_s and $\delta^{18}O_V$. In order to test the sensitivity of $\delta^{18}O_{trans}$ to variability in w_a/w_i, T_L, g_s and $\delta^{18}O_V$ we calculated $\delta^{18}O_{trans}$ from Eqn 5 using average input parameters that fell within the range of values observed in this study and in natural systems.

Table 1. Values for input parameters of the sensitivity analyses

	–50%	–25%	0	+25%	+50%
T_L (°C)	12	18	24	30	36
g_s (mol m^{-2} s^{-1})	0.15	0.21	0.3	0.39	0.45
w_a/w_i	0.25	0.375	0.50	0.625	0.75
Water vapour $\delta^{18}O$ (‰)	–25.5	–21.25	–17	–12.5	–8.5

In order to test the sensitivity of Eqn 5 to individual input parameters we varied each parameter by –50, –25, +25 and +50% while keeping the other parameters constant (Table 1). This analysis was repeated for different initial values of the input parameters in order to evaluate the interaction between parameters. For example, to test for the potential interactive effects between w_a/w_i and $\delta^{18}O_V$, we varied $\delta^{18}O_V$ by –50, –25, +25 and +50% for three different values of w_a/w_i.

RESULTS

Changes in the isotope ratio of background water vapour

The four leaves of WT38 tobacco showed gradual declines in assimilation rates during the measurement interval, which ranged from 250 to 300 min. At least some of this decline in A was due to slight declines in g_s in all leaves (Fig. 1a,b). Despite constant $\delta^{18}O$ of the water vapour being supplied to the leaf chamber during the first 90 min of measurement (Fig. 2a), all leaves showed marked variation in $\delta^{18}O_{trans}$, including an increase, on average, of about 6‰ (Fig. 2d). During this time, w_a/w_i and g_s increased to a stable value ~50–30 min before the step change in $\delta^{18}O_V$. After 90 min, $\delta^{18}O_{trans}$ of the leaves had begun to converge on the $\delta^{18}O$ of irrigation water (Fig. 2d).

After approximately 90 min, the leaf chamber inlet vapour source was changed so that inlet vapour was isotopically heavier than $\delta^{18}O_{trans}$. During this change, there were transient fluctuations in g_s and w_a/w_i (Fig. 1b,d). After the transient fluctuations had dissipated, w_a/w_i, g_s, T_L and by extension ε_k, and ε^+ were relatively constant for the first 55 min of measurement with the enriched inlet vapour (Figs 1b–d and 2b,c). In response to the shift in the isotopic difference between leaf water and background water vapour, $\delta^{18}O_{trans}$ for plants 1 and 2 displayed a slight step change towards depleted values (~2.8‰ less than irrigation water), as compared with the $\delta^{18}O_{trans}$ values measured with the first inlet vapour source. $\delta^{18}O_{trans}$ was relatively stable for all leaves during the 100 min with this isotopically heavier inlet vapour. The $\delta^{18}O_{trans}$ for plant 3 was slightly above irrigation water until the last 35 min when $\delta^{18}O_{trans}$ was equal to the irrigation water $\delta^{18}O$. Similarly the $\delta^{18}O_{trans}$ for plant 4 was greater than irrigation water, by 1.8‰, with a downward shift towards irrigation water ~35 min before changing back to the original vapour source. This depletion in $\delta^{18}O_{trans}$ for plants 3 and 4 coincided with a decline in w_a/w_i (Figs 1d & 2d).

After about 100 min at this isotopically heavy inlet vapour, the inlet vapour source was returned to the original source,

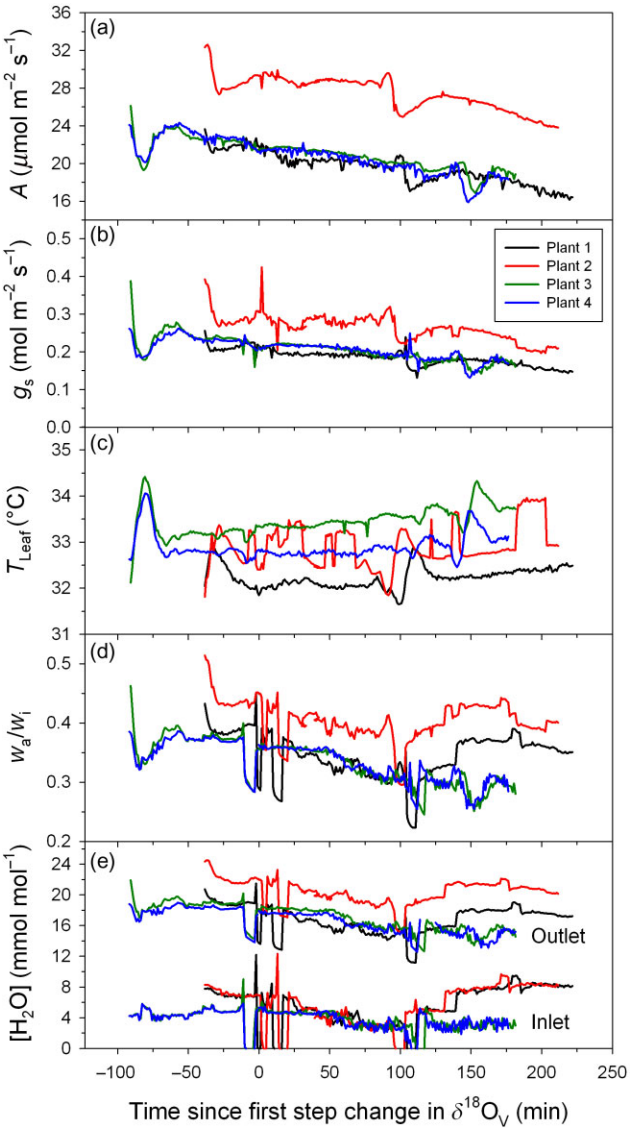

Figure 1. Gas exchange measurements during the step change in $\delta^{18}O$ of inlet vapour experiment with tobacco leaves. In (a) photosynthesis; (b) stomatal conductance; (c) leaf temperature; (d) the ratio of ambient and intercellular leaf water vapour mole fraction; and (e) the vapour concentration of leaf chamber inlet and outlet air streams. Values for plant 1 are shown in black, plant 2 red, plant 3 green and plant 4 blue.

which was isotopically much more depleted than $\delta^{18}O_{trans}$. During the switch to the original vapour, absolute humidity in the cuvette dropped temporarily, although g_s and the equilibrium and kinetic fractionations remained nearly constant. A and g_s declined slightly for all leaves (Fig. 1a,b) over the 100 min since the switch to the original vapour. In response to the change, $\delta^{18}O_{trans}$ showed a small increase in all leaves, of between 0.7 and 3‰ (Fig. 2d). After these initial effects, $\delta^{18}O_{trans}$ decreased during the final 50 min of measurement for three of the four leaves to end at similar values to the final measurement after the first step change and within 2.9‰ of irrigation water $\delta^{18}O$ (Fig 2d).

Changes in background CO_2 concentration

Upon initially inserting the WT38 tobacco leaves in the cuvette, we observed large shifts in $\delta^{18}O_{trans}$ and physiology as the leaves responded to cuvette conditions (both decreasing stomatal conductance, e.g. leaf 7, and increasing stomatal conductance, e.g. leaf 8). Cuvette conditions were likely very different from the conditions prior to insertion into the cuvette. At a c_a of 400 ppm, all four WT38 tobacco leaves had reached steady-state gas exchange with constant g_s and constant A for at least 5–10 min before the step change in c_a to 800 ppm (Fig. 3). The stable gas exchange conditions prior to the step change in c_a resulted in stable w_a/w_i, ε^+ and ε_k, and hence relatively constant $\delta^{18}O_{trans}$.

After 40 min at a c_a of 400 ppm, c_a was increased to 800 ppm. Within 2 min of this change, all leaves showed a reduced g_s and w_a/w_i, and reached a new stable g_s 10–30 min after this change (Fig. 3b). As expected, the lower values for stomatal conductance resulted in higher kinetic fractionation

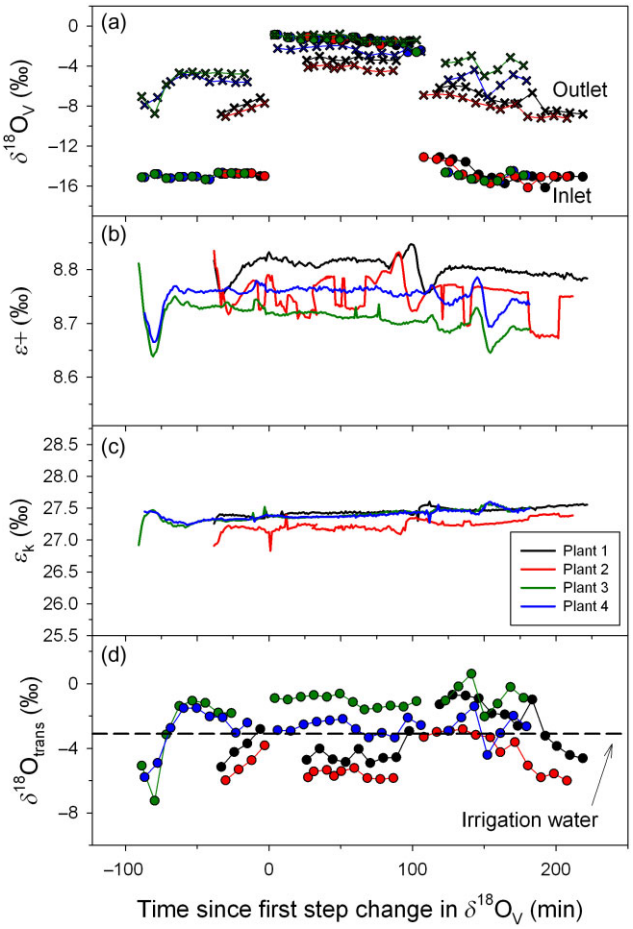

Figure 2. Measured and calculated stable oxygen isotope compositions (SMOW standard) of (a) the leaf chamber inlet and outlet air streams water vapour; (b) equilibrium vapour fractionation; (c) kinetic fractionation for $H_2{}^{18}O$; and (d) $\delta^{18}O$ of transpired vapour, during a step change in $\delta^{18}O$ of inlet vapour with tobacco leaves. Values for plant 1 are shown in black, plant 2 red, plant 3 green and plant 4 blue.

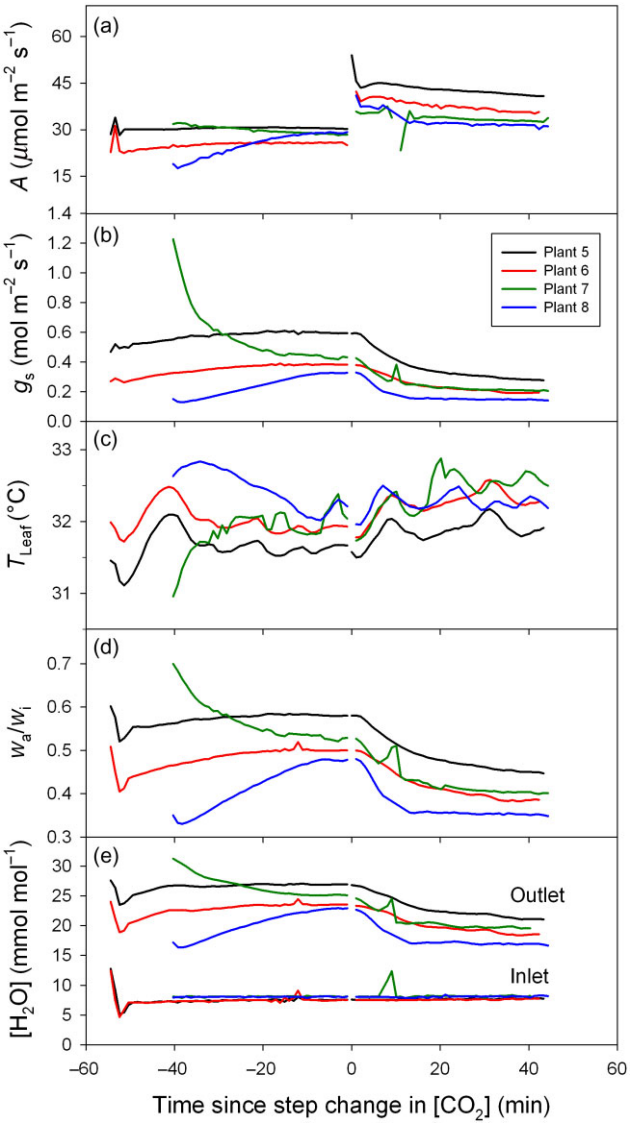

Figure 3. Gas exchange measurements before and after a step change in CO_2 concentration from 400 to 800 μmol mol^{-2}, for tobacco leaves. In (a) photosynthesis; (b) stomatal conductance; (c) leaf temperature; (d) the ratio of ambient to intercellular vapour pressures; and (e) the vapour concentration of leaf chamber inlet and outlet air streams. Values for plant 5 are shown in black, plant 6 red, plant 7 green and plant 8 blue.

(Fig. 4c), but equilibrium fractionation remained relatively constant because of minor variation in T_L (Figs 4b & 3c). All leaves showed a decline in $\delta^{18}O_{trans}$ in response to the increase in c_a, the timing of which approximately mirrored that of the decline in g_s. By approximately 30 min after the step change, $\delta^{18}O_{trans}$ from all leaves began to converge on similar values with three leaves having remarkably similar $\delta^{18}O_{trans}$ values. After the initial physiological response to the disturbance caused by changing c_a, both g_s and $\delta^{18}O_{trans}$ eventually converged on steady-state values. Final $\delta^{18}O_{trans}$ values for all leaves were within 3‰ of each other and within 1.7‰ of the irrigation water (Fig. 4d).

Similar to results from the WT38 tobacco leaves, gas fluxes from the *Citrus* leaves showed initial responses to cuvette conditions during the first 10 min of measurement at c_a of 400 ppm. During this time g_s, A, w_a/w_i and $\delta^{18}O_{trans}$ all increased (Figs 5a,b,d & 6d). By approximately 8 min before the step change in c_a from 400 to 730 ppm, g_s, w_a/w_i and A had reached stable values (Fig. 5a,b,d). While at physiological steady state before the step change in c_a, $\delta^{18}O_{trans}$ was stable and within 5‰ of source water. After the first step change in c_a, g_s and w_a/w_i immediately declined in all three *Citrus* leaves and continued to decline during the subsequent 20–30 min (Fig. 5b,d). In response to the first change in c_a, $\delta^{18}O_{trans}$ showed an immediate drop of 1–3‰ in 4 min, depending on the leaf (Fig. 6d). Similarly, ε_k increased for at least 10 min after the c_a change in response to the decrease in g_s (Fig. 6c). Despite the changes in g_s in response to the step change in c_a, T_L and thus the equilibrium fractionation factor, ε^+, did not respond to this step change instead, ε^+ declined steadily (Figs 6b & 5c).

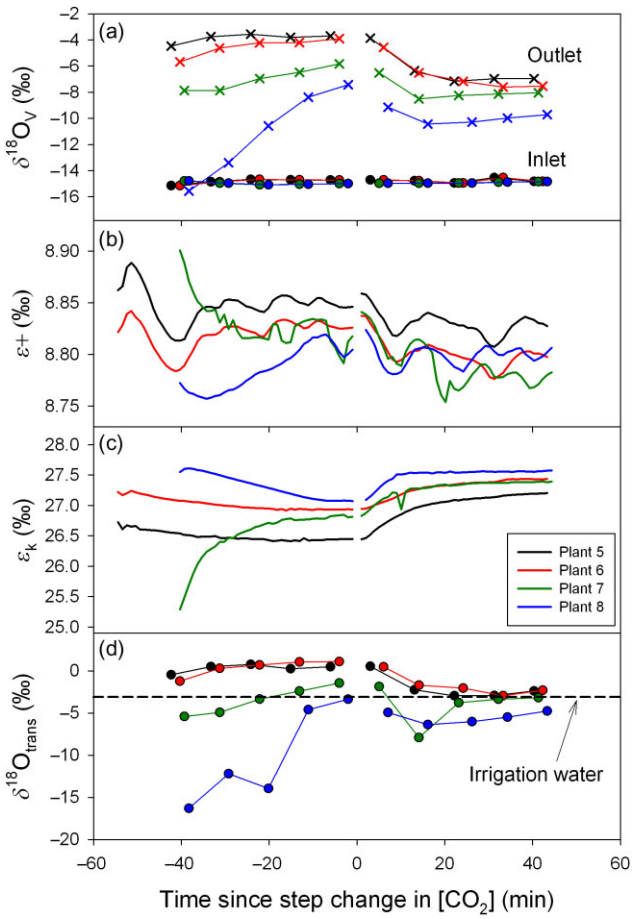

Figure 4. Measured and calculated stable oxygen isotope compositions (SMOW standard) of (a) the leaf chamber inlet and outlet air streams water vapour; (b) equilibrium vapour fractionation; (c) kinetic fractionation for $H_2{}^{18}O$; and (d) $\delta^{18}O$ of transpired vapour, during the step change in CO_2 concentration with tobacco leaves. Values for plant 5 are shown in black, plant 6 red, plant 7 green and plant 8 blue.

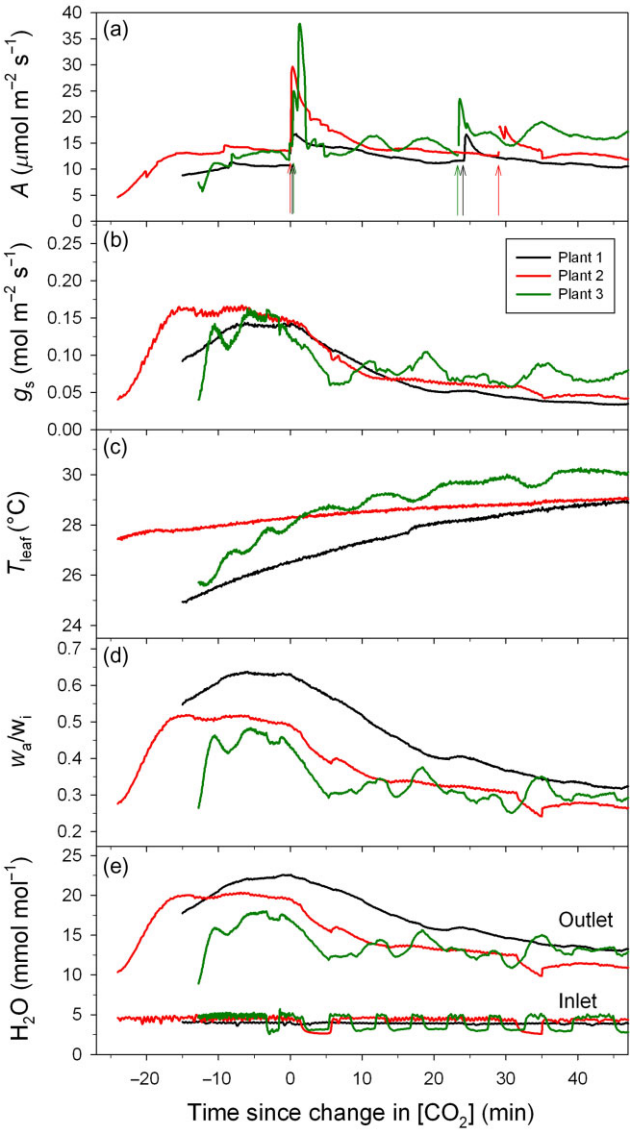

Figure 5. Gas exchange measurements during a series of step changes in CO_2 concentration; from 400 to 730 μmol mol^{-1} (step change at time zero), then to 900 μmol mol^{-2} (step change indicated by coloured arrow) for *Citrus* leaves. In (a) photosynthesis; (b) stomatal conductance; (c) leaf temperature; (d) the ratio of ambient to intercellular vapour pressure; and (e) the vapour concentration of leaf chamber inlet and outlet air streams. Values for leaf 1 are shown in black, leaf 2 red and leaf 3 green.

The second c_a concentration of 730 ppm was maintained for 22–30 min. In the last 10 min of this time period, the leaves showed stable g_s, T_L and w_a/w_i (Fig. 5b–d), although $\delta^{18}O_{trans}$ was still declining away from the $\delta^{18}O$ of source water for all three leaves. The second c_a change to 900 ppm caused sudden increases in A, although A quickly declined to its previous values (Fig. 5a). In two of the leaves, g_s continued to decline slightly and reached stable values 10–15 min after this second c_a change (Fig. 5b). After the second c_a change, $\delta^{18}O_{trans}$ for plants 1 and 2 were stable as was g_s, T_L, w_a/w_i, ε_k and ε^+ (Figs 5b–d & 4b–d). Leaf 3 showed greater variation in g_s, T_L, w_a/w_i, ε_k and ε^+ after the second change, and this variability was also reflected in $\delta^{18}O_{trans}$ (Figs 5b–d & 6b–d).

Changes in the rate of change of leaf water isostorage in response to changes in c_a

Variation in the rate of change in leaf isostorage, in response to a step change in c_a, differed between the two species and among plants within each species. Despite constant E prior to the step change in c_a, the rate of change in leaf isostorage for *Citrus* plant 1 decreased, from 8.3 to 2.6 mmol m^{-2} s^{-1}‰ because of an increase in Δ_{trans} (Fig. 7a–c). *Citrus* plant 2 showed the opposite trend with the rate of change in leaf isostorage increasing from 11.2 to 18.1 mmol m^{-2} s^{-1}‰, despite relatively stable Δ_{trans} (–7.7 to –6.5‰) because of an approximate doubling of the transpiration rate from 1.4 to 2.7 mmol m^{-2} s^{-1} (Fig. 7a–c). Because of a 1.9‰ increase in Δ_{trans} from –7.2 to –5.1‰ (Fig. 7a–c), the rate of change in leaf

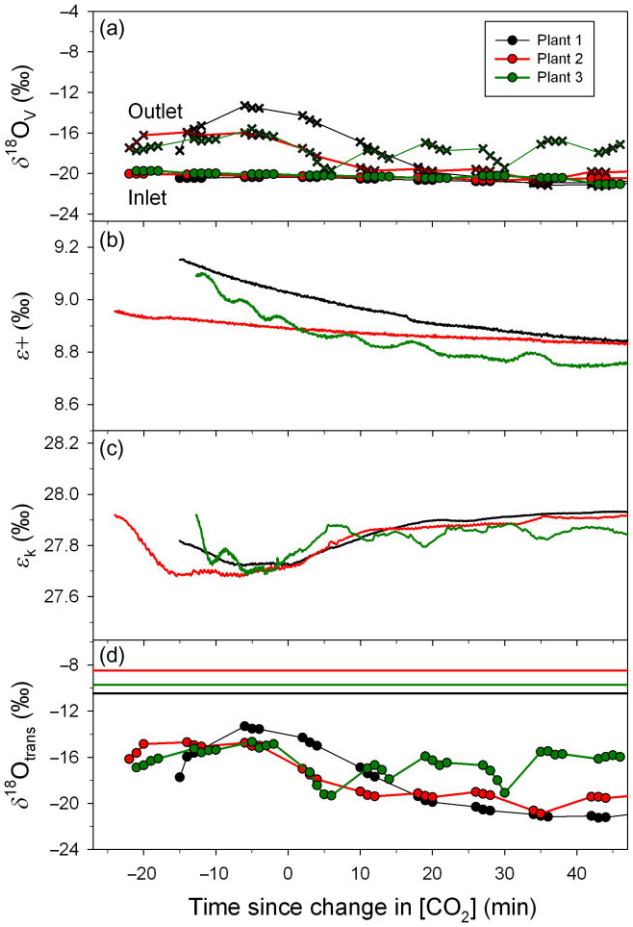

Figure 6. Measured and calculated stable oxygen isotope compositions (SMOW standard) of (a) the leaf chamber inlet and outlet air streams water vapour; (b) equilibrium vapour fractionation; (c) kinetic fractionation for $H_2{}^{18}O$; and (d) $\delta^{18}O$ of transpired vapour, during a series of step changes in CO_2 concentration with *Citrus* leaves. Values for leaf 1 are shown in black, leaf 2 red and leaf 3 green. Solid lines in D represent the ^{18}O composition of xylem source water.

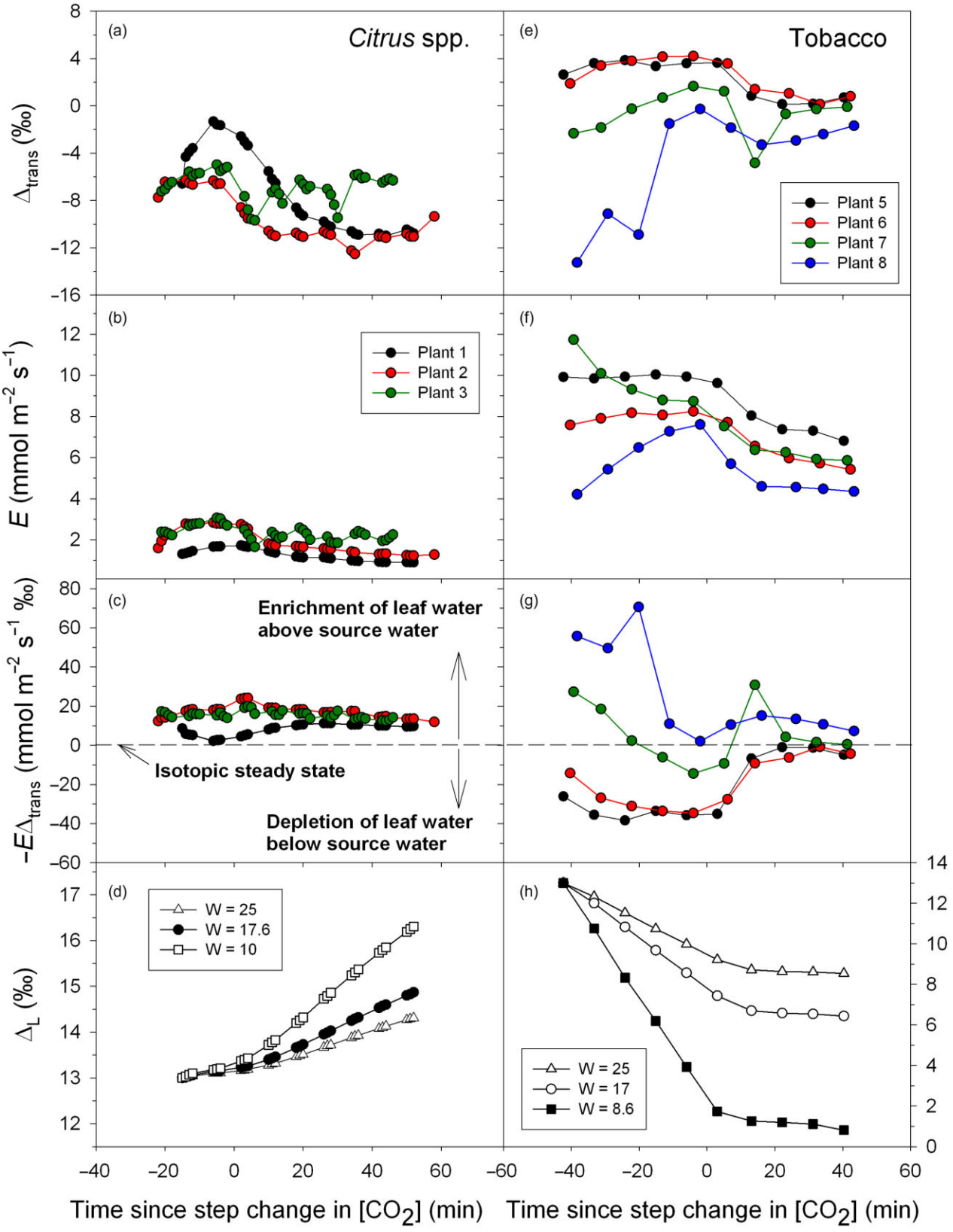

Figure 7. Gas exchange measurements and the measured and modelled stable oxygen isotope enrichment of transpiration, the transpiration isoflux, and leaf water enrichment before and after a step change in CO_2 concentration from (a–d) 400 to 730 μmol mol^{-1} for *Citrus* and (e–h) 400 to 800 μmol mol^{-1} for tobacco. In (a & e) the enrichment of transpiration above source water; (b & f) transpiration; (c & g) the transpiration isoflux; and (e & f) modelled leaf water enrichment above source water for three different leaf water contents.

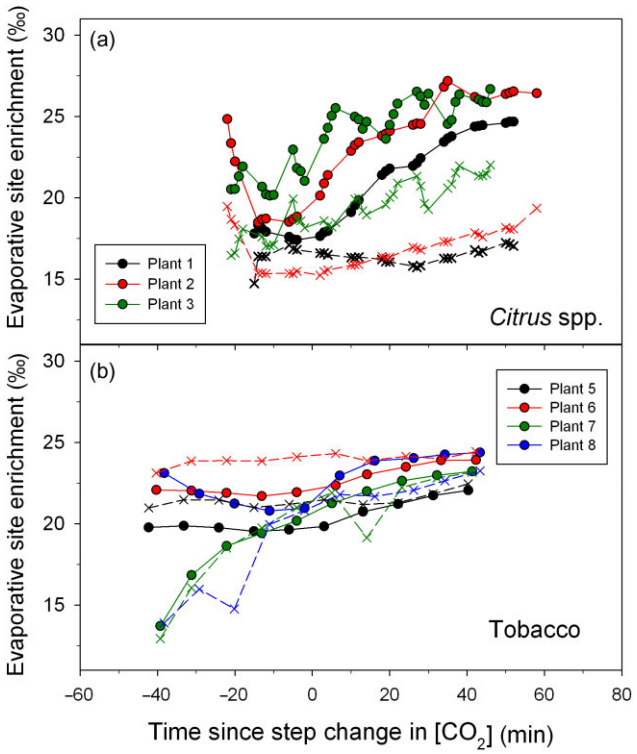

Figure 8. Steady-state (Δ_{es}) and non steady-state (Δ_e) predictions of leaf water enrichment above source water at the evaporation site for (a) *Citrus* and (b) tobacco in response to a step change in CO_2 concentration (as described in Figure 7). Values for Δ_{es} are shown as filled circles with values for Δ_e as X.

isostorage for *Citrus* plant 3 showed a decrease from 17.3 to 13.9 mmol m^{-2} s^{-1}‰ despite a relatively stable E.

After the step change in c_a, from 730 to 900 ppm all three *Citrus* plants showed an immediate increase in the rate of change in leaf isostorage (Fig. 7c), because of steady decreases in Δ_{trans} during the first 20–30 min after the step change in c_a (Fig. 7a) combined with a steady decrease in E (Fig. 7b). For tobacco plants 5, 6 and 7, after the step change in c_a, there was an overall decrease in the rate of change in leaf isostorage because of decreases in both Δ_{trans} and E (Fig. 7e–g). The rate of change in leaf isostorage for plant 8 initially increased after the step change in c_a and then decreased towards ISS (Fig. 7g). This variation in the rate of change in leaf isostorage was associated with an overall decrease in E, and an initial decrease and then increase in Δ_{trans} (Fig. 7e & f).

Using the rate of change in leaf isostorage data from *Citrus* plant 1 and tobacco plant 5, we modeled the sensitivity of leaf water enrichment to variation in leaf water content (i.e. W) over time. The absolute increase (i.e. *Citrus* plant 1) or decrease (i.e. tobacco plant 5) in Δ_L decreased as W increased. For *Citrus* leaf 1, during the ~70 min of the CO_2 manipulation experiment, the absolute modeled increase in Δ_L was 3.3, 1.8 and 1.3‰ for W of 10, 17.6, and 25 mol m^{-2}, respectively (Fig. 7d). For tobacco leaf 5, during the ~80 min of the CO_2 manipulation experiment, the absolute modeled decrease in Δ_L was 12.2, 6.6 and 4.5‰; and for W of 8.6, 17 and 25 mol m^{-2} (Fig. 7h).

Using Eqn 7, we evaluated differences between steady-state and non–steady-state predictions of $\Delta^{18}O$ of leaf water at the evaporation site. Prior to the step change in c_a, model predictions of Δ_{es} exceeded Δ_e by 0.6–5.4‰ (Fig. 8a) because $\delta^{18}O_{trans}$ values less than stem xylem water for *Citrus* plants (Figs 6d & 7a). Similarly, after the step change in c_a, model predictions of Δ_{es} exceeded Δ_e by 1–9.8‰ (Fig. 8a) because of $\delta^{18}O_{trans}$ values that remained less than stem xylem water for the *Citrus* plants (Figs 6d & 7a). For the tobacco plants model predictions of Δ_{es} were both greater than and less than than Δ_e. Prior to the step change in c_a, the model predictions of Δ_{es} were less than Δ_e by 1–2‰ (Fig. 8b) because of $\delta^{18}O_{trans}$ values that were greater than irrigation water (Figs 4d & 7e). Plants 7 and 8 showed the opposite trend with Δ_{es} exceeding Δ_e by 0.7–9.2‰. After the step change in c_a differences between Δ_{es} and Δ_e ranged from ~0.1 to 2.2‰.

In order to test for variation in the effective path length, we used data obtained from *Citrus* plant 1 during the c_a manipulation experiment. As shown in Fig. 9, after the initial response to being placed in the leaf chamber and prior to the step change in c_a, the difference between steady-state and non–steady-state model predictions of the effective path length ($L_S - L_{NS}$) were relatively constant for a given Δ_L. After the step change in c_a, the difference between L_S and L_{NS} increased until ~40 min after the change in c_a when a stable $-E\Delta_{trans}$ was reached. Once $-E\Delta_{trans}$ was stable the difference between L_S and L_{NS} stabilized (Figs 7d and 9).

According to the Craig and Gordon model sensitivity analysis all input parameters had a substantial direct effect on $\delta^{18}O_{trans}$, except for g_s (Fig. 10). Variation in w_a/w_i and $\delta^{18}O_V$ had the greatest direct effect on $\delta^{18}O_{trans}$. We also observed strong interactive effects between w_a/w_i and T_L and w_a/w_i and $\delta^{18}O_V$. As w_a/w_i increased the influence of variation in T_L on $\delta^{18}O_{trans}$ increased, the same was true for $\delta^{18}O_V$

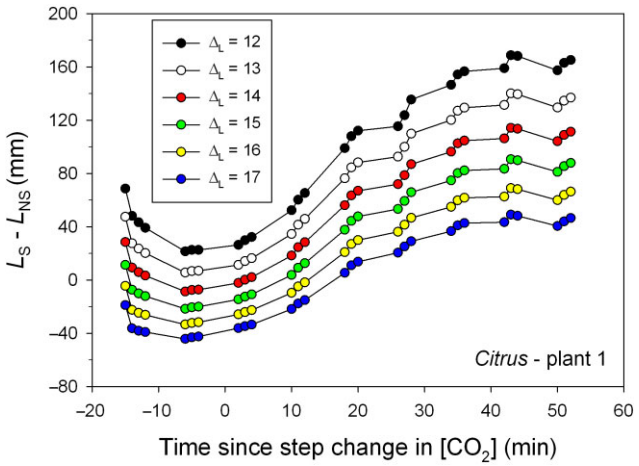

Figure 9. The difference between steady-state and non–steady-state model predictions for the effective path length for *Citrus* plant 1 during the CO_2 manipulation experiment. Model predictions were made across a range of leaf water ^{18}O enrichment 'starting points'.

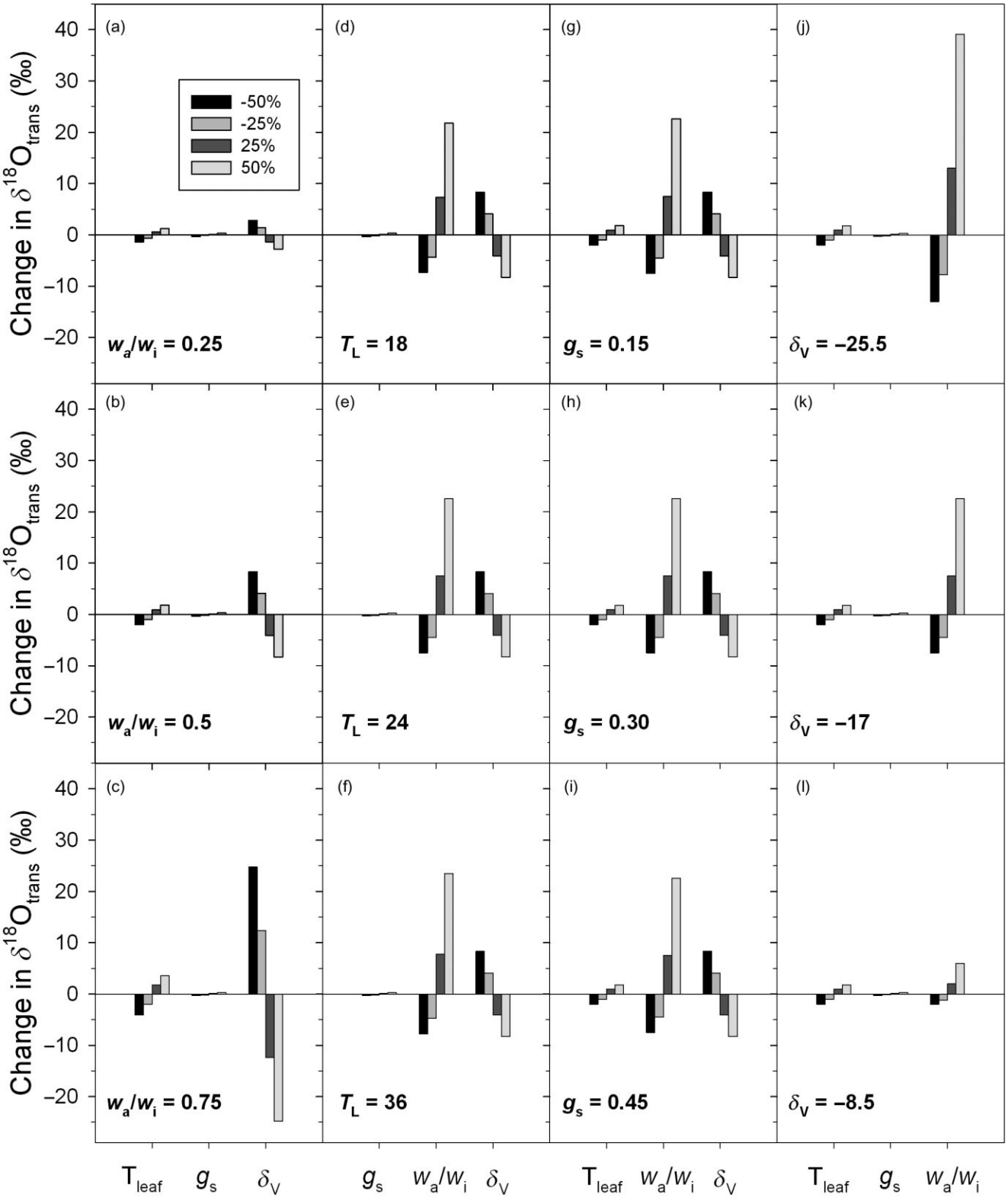

Figure 10. Results for the sensitivity analyses using the Craig and Gordon evaporation model (Eqn 5) and input parameters shown in Table 1. Each input parameter was independently varied by ±25% and ±50% while other parameters were held constant at three different levels. This allowed us to test for interactions between input parameters. T_{leaf} is leaf temperature in degrees C, g_s is stomatal conductance (mol m^{-2} s^{-1}); w_a and w_i are the mole fractions (mol mol^{-1}) of water vapour in the ambient atmosphere and inside the leaf, and δ_v is the 18O isotope composition of ambient water vapour.

(Fig. 10a–c). Further, as δ_V increased the influence of w_a/w_i decreased (Fig. 10j–l).

Leaf water residence times

Citrus leaves had almost twice the water concentration as tobacco leaves (17.6 ± 2.9 mol m^{-2} compared with 8.68 ± 0.51 mol m^{-2}) and also longer leaf water residence times. In fact, leaf water residence times for the two species differed by an order of magnitude. The average leaf water residence time for the *Citrus* leaves was 303 ± 230 min with a minimum of 99 min when leaf surface conductance was at a maximum of 0.125 mol m^{-2} s^{-1} and a maximum leaf water residence time of 769 min when stomatal conductance was at a minimum of 0.03 mol m^{-2} s^{-1}. The average leaf water residence time for the tobacco leaves was 36 ± 15 min. Similar to the *Citrus* leaves, the shortest residence time, 9 min, occurred when stomatal conductance was at a maximum of 0.59 mol m^{-2} s^{-1}, while the longest residence time for tobacco, 57 min, occurred when stomatal conductance was at a minimum of 0.15 mol m^{-2} s^{-1}.

DISCUSSION

Integration of measurements of water vapour isotopes and gas exchange fluxes

Our modifications of both gas exchange systems (Supporting Information Figs S1 and S2) to include the vapourization module allowed the manipulation of absolute humidity across a wide range of water vapour concentrations without isotopic fractionation. Traditional methods used in gas exchange systems control cuvette humidity either by chemically scrubbing out ambient water (LI-6400) or by bubbling air through water (MPH-1000), both of which can cause fractionation and produce variable isotope ratios of the background water vapour. The equilibrium fractionation factor ($\varepsilon+$) can be used to predict the isotope ratios of air bubbled through water if the surface temperature of the water is known (Hendry, Richman & Wassenaar 2011). However our modified gas exchange systems, which now include the vapourization module, represent a substantial improvement for measuring isotope fluxes because we can control water vapour concentration and isotope ratios independently of one another. This allows greater experimental control and will enable improved testing of the abiotic and biotic factors contributing to variation in the isotope compositions of leaf water and of transpiration (see Eqn 3).

$\delta^{18}O_{trans}$ and the rate of change in leaf isostorage

The environmental conditions under which ISS transpiration occurs at the leaf level have rarely been directly addressed. Wang & Yakir (1995) suggested that ISS transpiration may be rare in naturally varying conditions, and subsequent work under field conditions has largely supported this idea (Harwood *et al*. 1998, 1999). In natural settings $\delta^{18}O_V$, w_a/w_i, as well as the equilibrium ($\varepsilon+$) and diffusive (ε_k) fractionation factors, can vary greatly over a diurnal cycle. As our results show, changes in these abiotic and biotic conditions can cause large and sustained changes in $\delta^{18}O_{trans}$. These changes are expected to persist until sufficient time has passed under constant environmental and physiological conditions to allow the $\delta^{18}O_{trans}$ to relax to that of the xylem water supplying transpiration (i.e. until $R_{trans} \approx R_S$ in Eqn 1). The prolonged deviation of $\delta^{18}O_{trans}$ from $\delta^{18}O_S$ observed here suggests that the residence time of the water pool supporting the transpiration flux is longer than the timescales over which w_a, w_i, ε_k, $\varepsilon+$ and R_v varied in our experiments. Indeed, the residence time of leaf water may be longer than the timescales over which these variables may change under natural conditions.

During the CO_2 manipulation experiment we observed changes in $\delta^{18}O_{trans}$ that tracked changes in w_a/w_i, T_L and g_s. According to the Craig and Gordon model sensitivity analysis, the observed variation in $\delta^{18}O_{trans}$ was likely associated with variation in w_a/w_i and T_L with little direct influence of ε_k, i.e. g_s (Fig. 10). The Craig and Gordon model for evaporation (Eqns 3 & 5) predicts changes in $\delta^{18}O_{trans}$ to be positively correlated with w_a/w_i and T_L (Fig. 10d–f). However, changes in $\delta^{18}O_E$ in response to variation in T_L are expected to be much less than those associated with variation in w_a/w_i with the overall effect of T_L increasing as w_a/w_i increases (Fig. 10a–c). As predicted by the model sensitivity analysis, during periods when w_a/w_i was relatively low, variation in w_a/w_i determined the overall direction of change in $\delta^{18}O_{trans}$ for the *Citrus* and tobacco plants. Further, when w_a/w_i was relatively high the influence of variation in T_L on $\delta^{18}O_{trans}$ was more pronounced. For example, for both the *Citrus* and tobacco plants, when w_a/w_i was relatively low a ~0.15 decrease in w_a/w_i resulted in a decrease in $\delta^{18}O_{trans}$ despite an increase in T_L by 1–3 °C (Figs 5c,d & 6d). Additionally, for tobacco plant 7 when w_a/w_i was relatively high a 0.10 decrease in w_a/w_i, as T_L increased by 1 °C, had no observable change in $\delta^{18}O_{trans}$ (Figs 3c, d & 4d). Taken together these results provide strong support for the interactive effects of w_a/w_i and T_L as predicted by the Craig and Gordon model sensitivity analysis.

Current leaf water enrichment models suggest that after a change in w_a/w_i, $\varepsilon+$ and ε_k the rate of change in leaf water isostorage for a species with a short leaf water residence time should approach zero faster than a species with a long leaf water residence time (Dongmann *et al*. 1974; Farquhar & Cernusak 2005). As shown by Eqn 12, isotope models that incorporate leaf water residence time often treat transpiration as coming from a single reservoir of water, that is bulk leaf water, such that leaf water content divided by the one-way flux of water from the leaf (i.e. gw_i in Eqn 12) can be used to describe leaf water residence time. Other studies have suggested that transpired water is derived from multiple pools of water that vary in their sizes and relative contributions to the transpiration stream (Cruiziat *et al*. 1980; Tyree *et al*. 1981; Yakir *et al*. 1989, 1990; Wang & Yakir 1995; Zwieniecki, Brodribb & Holbrook 2007). In the current study we are unable to determine if deviations from ISS are associated with multiple pools of water in leaves. However, our data clearly show that changes in T_L, w_a/w_i and g_s have

long-lasting effects on $\delta^{18}O_{trans}$ for the two species in this study. Furthermore, the presence of stable $\delta^{18}O_{trans}$ that differs from $\delta^{18}O_S$ could result from stable proportional contributions to the transpiration stream by multiple leaf water pools that differ in their isotopic compositions. An unchanging proportional contribution from an isotopically distinct second pool of water may cause a constant offset of $\delta^{18}O_{trans}$ from $\delta^{18}O_S$ (e.g. tobacco plants 5 & 6 in Fig. 4d just before the step change or citrus plants 1 & 2 in Fig. 6d at the end of the experiment). If leaf water is composed of multiple pools, each with unique isotope compositions, then modeling leaf water residence time requires more complexity than the single pool model that is frequently applied. Further evaluations of leaf water residence time are necessary to determine to what extent hydraulic compartmentalization exists in leaves in order to account for the dynamic variation of $\delta^{18}O_{trans}$ in response to changes in w_a/w_i, ε_k, $\varepsilon+$, and the isotope difference from leaf to air.

Using the $\delta^{18}O$ of stem xylem water as source water for the *Citrus* plants and irrigation water as source water for the tobacco plants, we evaluated changes in the transpiration isoflux (i.e. $E\Delta_{trans}$) in response to variation in w_a/w_i, $\varepsilon+$ and ε_k that was triggered by a step change in c_a (i.e. c_a step change depicted in Figs 3 & 5). Our data from the CO_2 manipulation experiments provide further support that in a variable environment, when w_a/w_i, $\varepsilon+$ or ε_k are not constant, the time required to re-establish ISS transpiration (i.e. $E\Delta_{trans} = 0$) is greater for species with relatively long leaf water residence times, as predicted by a single pool leaf water residence model (Eqn 12). The shorter leaf water residence times, predicted by Eqn 12, for tobacco (9–57 min) compared with those of *Citrus* (99–769 min) corresponded with a more rapid approach of the tobacco transpiration isoflux to zero after a change to a new, relatively stable, w_a/w_i, $\varepsilon+$ and ε_k (Fig. 7c,g).

Additionally, assuming all water in the leaf contributes equally to the leaf transpiration stream we used Eqn 2 and measured values of the transpiration isoflux to evaluate the influence of variable leaf water content on leaf water enrichment. Our model results suggest that the absolute increase or decrease in leaf water enrichment in response to variation in the leaf transpiration isoflux is sensitive to variation in leaf water content. As shown in Fig. 7d, increasing W of *Citrus* plant 1 by 42%, from 17.6 to 25 mol m^{-2}, resulted in a 38% decrease in the magnitude of leaf water enrichment as $-E\Delta_{trans}$ became more positive (Fig. 7c,d). Similarly, increasing W of tobacco plant 1 from 17 to 25 mol m^{-2} resulted in a 32% increase in leaf water enrichment as $-E\Delta_{trans}$ became less negative (Fig. 7g,h). Our model results of the effects of W on Δ_L are consistent with previous measurements of leaf water enrichment. For example, the modeled change in leaf water enrichment for tobacco ($W = 17$ mol m^{-2}) was similar to the magnitude of change observed for field-grown lupin, which had similar transpiration rates, w_a/w_i, and leaf water content (Cernusak *et al*. 2002).

In response to changes in $\delta^{18}O_V$ the observed changes in $\delta^{18}O_{trans}$ followed that expected from Craig and Gordon model predictions (i.e. Eqns 3 & 5). When the tobacco leaves were exposed to a ~15‰ increase in the $\delta^{18}O$ of water vapour entering the leaf cuvette there was an immediate, rapid decline in $\delta^{18}O_{trans}$ by 1–3‰ for all, but one of the tobacco plants. This change in $\delta^{18}O_{trans}$ occurred during relatively stable w_a/w_i, $\varepsilon+$ and ε_k. According to the Craig and Gordon model of evaporation (Eqn 3) when the equilibrium and kinetic fraction factors and w_a/w_i are constant, an increase in the heavy isotope composition of atmospheric water vapour (R_V in Eqn 3) should cause a decrease in the heavy water isotope composition of transpiration (R_{trans} in Eqn 3). Similar to T_L, the sensitivity of $\delta^{18}O_{trans}$ to a change in the isotope composition of atmospheric water vapour (i.e. $\delta^{18}O_V$) is ultimately a function of w_a/w_i and the absolute change in $\delta^{18}O_V$ (Fig. 10). As w_a/w_i increases or the absolute change in $\delta^{18}O_V$ increases the greater the effect of a variable $\delta^{18}O_V$ on $\delta^{18}O_{trans}$. Similar to these model predictions the observed changes in the $\delta^{18}O_{trans}$ of tobacco was greater when w_a/w_i and the absolute change in $\delta^{18}O_V$ was greater (Figs 1d & 2a,d). For example tobacco plant 2 showed the greatest change in $\delta^{18}O_{trans}$ when the $\delta^{18}O_V$ of the water vapour entering the leaf cuvette was changed. Plant 2 also had the highest w_a/w_i (Fig. 1d) and experienced the greatest absolute change in the $\delta^{18}O_V$ that transpiration was mixing into (Fig. 2a). The $\delta^{18}O_{trans}$ of plants 3 and 4 were the least sensitive to the change in the $\delta^{18}O_V$ of the water vapour entering the leaf cuvette and they were the plants with the lowest w_a/w_i and absolute change in the $\delta^{18}O_V$ that transpiration was mixing into.

Taken together, the results from the CO_2 and $\delta^{18}O_V$ manipulation experiments highlight how leaf physiological responses to step changes in environmental variables and to the isotope composition of atmospheric humidity can result in non–steady-state transpiration isoflux. It is important to note that during our measurements, the Li6400xt cuvettes did not entirely enclose the tobacco leaves. For most of these measurements, the cuvette was placed near the tips of the leaves, potentially allowing for progressive evaporative enrichment of the xylem source water along the length of the leaf (Wang & Yakir 1995; Helliker & Ehleringer 2000; Gan *et al*. 2003). In some of our measurements, particularly those under changing c_a, $\delta^{18}O_{trans}$ was isotopically more enriched than irrigation water, consistent with progressive enrichment of the xylem source water feeding the evaporation site along the leaf axis (Figs 2d & 4d). Because we do not know the $\delta^{18}O$ of the xylem water for the portion of the leaf inside the cuvette, we were not able to determine unequivocally when the tobacco leaves were in ISS. Nonetheless, the rapid, dynamic responses of $\delta^{18}O_{trans}$ to changes in cuvette conditions highlight when transpiration was most likely not in ISS. These results build upon previous work suggesting that transpiration is rarely in ISS when leaves are exposed to a variable environment (Wang & Yakir 1995; Harwood *et al*. 1998, 1999).

Differences between steady-state and non–steady-state model predictions of Δ_e and L

Several recent studies suggest that non-steady state leaf water models are necessary when evaluating ^{18}O discrimination

during photosynthesis due to large differences between steady-state (Δ_{es}) and non steady-state (Δ_e) model predictions of the ^{18}O composition at the evaporation site in leaves. For example, previous research characterizing daytime variation in the ^{18}O composition of ecosystem evapotranspiration ($\delta^{18}O_{ET}$) suggests that Δ_{es} can be as much as 2‰ less than Δ_e calculated from $\delta^{18}O_{ET}$ (Welp *et al*. 2008). Additionally, assuming $\delta^{18}O_v$ is in isotopic equilibrium with precipitation, daytime variation in the ^{18}O composition of leaf water suggests that Δ_{es} can be 5‰ or more above Δ_e (Seibt *et al*. 2006). Our observations of the isotope composition of transpiration provide further support for the suggestion that non–steady-state models are necessary to accurately predict ^{18}O enrichment at the evaporation site in leaves. Similar to Welp *et al*. (2008), we show that Δ_{es} for tobacco plants 5 and 6 was up to 2‰ less than Δ_e, whereas Δ_{es} for the *Citrus* plants and tobacco plants 3 and 4 exceeded Δ_e by up to 8‰. As mentioned previously, because the Li6400xt cuvettes did not entirely enclose the tobacco leaves, it is likely that we underestimated the isotope composition of source water for use in the calculation of Δ_{es}. This inability to accurately characterize tobacco source water could result in model predictions of Δ_{es} that are less than Δ_e.

Additionally, large differences between Δ_{es} and Δ_e should result in large differences between steady-state and non–steady-state model predictions of the effective path length for water transport in leaves (L). The observed link between leaf hydraulic architecture and carbon gain (Brodribb *et al*. 2005; Franks 2006; Brodribb, Feild & Jordan 2007) has led to the suggestion that variation in the effective path length for water transport in leaves could provide important insights into other leaf physiological properties (e.g. Ferrio *et al*. 2012). Assuming Eqn 8 holds when the transpiration isoflux is not equal to 0 (i.e. $E\Delta_{trans} < \text{or} > 0$), we used our observations of $\delta^{18}O_{trans}$ to evaluate differences between steady-state and non–steady-state model predictions of the effective path length (L_S and L_{NS}, respectively). Our experimental setup did not allow us to characterize the ^{18}O composition of transpiration and bulk leaf water at the same time. As such, we evaluated differences between L_S and L_{NS} across a range of leaf water ^{18}O compositions. Across all values of bulk leaf water $\delta\ ^{18}O$, the difference between L_s and L_{ns} increased as Δ_{trans} decreased or the difference between R_{trans} and R_S increased. The large differences between steady-state and non–steady-state model predictions of the effective path observed here suggest that attempts to link variation in L using Eqn 8, both within and between species, to other leaf physiological properties would require knowledge of Δ_{trans}.

Implications for ecosystem–atmosphere water vapour and CO_2 exchange

These results also have important implications for scaling leaf level measurements to the ecosystem scale. The ubiquity of eddy covariance measurements in natural systems has facilitated high temporal resolution monitoring of water fluxes in natural systems (e.g. Tenhunen *et al*. 1998; Fisher *et al*. 2009). A desire to better understand the terrestrial water cycle has led many researchers to use stable isotopes to partition evapotranspiration among different ecosystem components. Partitioning using isotopes requires two isotopically distinct end member values (i.e. transpiration and evaporation). As previously discussed, common applications of this method assume that plant-transpired water is isotopically equivalent to xylem water in order to calculate the transpiration end member (Yepez *et al*. 2003; Williams, Cable & Hultine 2004). Yet our findings, in conjunction with previous studies, demonstrate that plant transpiration either is often not in ISS or can take over an hour of physiologically stable conditions to reach ISS (Wang & Yakir 1995; Harwood *et al*. 1998, 1999). Therefore, while a number of studies have used isotopes of CO_2 to partition ecosystem CO_2 fluxes (e.g. Pataki *et al*. 2003), our results raise questions about the applicability of this approach to partitioning ecosystem water fluxes over short time intervals. A combination of isoflux modeling in the non–steady-state and ecosystem-scale measurements using either the flux gradient method (e.g. Lee *et al*. 2005; Welp *et al*. 2008) or eddy covariance (Griffis *et al*. 2011) may offer a solution for ET partitioning when $\delta^{18}O_{trans}$ is not occurring at ISS.

ACKNOWLEDGMENTS

We would like to thank Greg Goldsmith and Lucas Cernusak for help with data collection and Hilary Stuart-Williams for loaning us his Picarro isotope analyser. Thanks to John Evans and Susanne von Caemmerer for sharing Eqn 11 and to Graham Farquhar and two anonymous reviewers for comments that greatly improved the paper. This research was supported in part by the 'HydroWatch' award made to UC Berkeley from the Keck Foundation. ABR was supported by the U.S. Department of Energy (DOE) Office of Science Graduate Fellowship Program, managed by Oak Ridge Associated Universities under contract number DE-AC05-06OR23100. MMB acknowledges support from the Australian Research Council (FT0992063 and DP110104269).

REFERENCES

Allison G.B., Gat J.R. & Leaney F.W.J. (1985) The relationship between deuterium and oxygen-18 Δ-values in leaf water. *Chemical Geology* **58,** 145–156.

Barbour M.M., Schurr U., Henry B.K., Wong S.C. & Farquhar G.D. (2000) Variation in the oxygen isotope ratio of phloem sap sucrose from Castor Bean. Evidence in support of the Péclet effect. *Plant Physiology* **123,** 671–679.

Barbour M.M., Farquhar G.D., Hanson D.T., Bickford C.P., Powers H. & McDowell N.G. (2007) A new measurement technique reveals temporal variation in $\delta^{18}O$ of leaf-respired CO_2. *Plant, Cell & Environment* **30,** 456–468.

Bariac T., Rambul S., Jusserand C. & Berger A. (1989) Evaluating water fluxes of field-grown alfalfa from diurnal observations of natural isotope concentrations, energy budget and ecophysiological parameters. *Agricultural and Forest Meteorology* **48,** 263–283.

Barkan E. & Luz B. (2007) Diffusivity fractionations of $H_2^{16}O/H_2^{17}O$ and $H_2^{16}O/H_2^{18}O$ in air and their implications for isotope hydrology. *Rapid Communications in Mass Spectrometry* **21,** 2999–3005.

Brodribb T.J., Holbrok N.M., Zwieniecki M.A. & Palma B. (2005) Leaf hydraulic capacity in ferns, conifers and angiosperms: impacts on photosynthetic maxima. *New Phytologist* **165,** 839–846.

Brodribb T.J., Feild T.S. & Jordan G.J. (2007) Leaf maximum photosynthetic rate and venation are linked by hydraulics. *Plant Physiology* **104,** 1890–1898.

Cernusak L.A., Pate J.S. & Farquhar G.D. (2002) Diurnal variation in the stable isotope composition of water and dry matter in fruiting *Lupinus angustifolius* under field conditions. *Plant, Cell & Environment* **25,** 893–907.

Ciais P., Denning A.S., Tans P.P., *et al.* (1997) A three-dimensional synthesis study of $\delta^{18}O$ in atmospheric CO_2 1. Surface fluxes. *Journal of Geophysical Research* **102,** 5857–5872.

Craig H. & Gordon L.I. (1965) Deuterium and oxygen-18 variations in the ocean and the marine atmosphere. In *Proceedings of a Conference on Stale Isotopes in Oceanographic Studies and Palaeotemperautres* (ed. E. Tongiorgi), pp. 9–130. Lischi and Figli, Pisa, Italy.

Cruiziat P., Tyree M.T., Bodet C. & LoGullo M.A. (1980) The kinetics of rehydration of detached sunflower leaves following substantial water loss. *New Phytologist* **84,** 293–306.

Dongmann G., Nurnberg H.W., Förstel H. & Wagener K. (1974) On the enrichment of $H_2{}^{18}O$ in the leaves of transpiring plants. *Radiation and Environmental Biophysics* **11,** 41–52.

Farquhar G.D. & Cernusak L.A. (2005) On the isotopic composition of leaf water in the non-steady state. *Functional Plant Biology* **32,** 292–303.

Farquhar G.D. & Lloyd J. (1993) Carbon and oxygen isotope effects in the exchange of carbon dioxide between terrestrial plants and the atmosphere. In *Stable Isotopes and Plant Carbon-Water Relations* (eds J.R. Ehleringer, A.E. Hall & G.D. Farquhar), pp. 47–70. Academic Press, London.

Farquhar G.D., Hubick K.T., Condon A.G. & Richards R.A. (1989) Carbon isotope discrimination and water-use efficiency. In *Stable Isotopes in Ecological Research* (eds P.W. Rundel, J.R. Ehleinger & K.A. Nagy), pp. 21–46. Springer-Verlag, New York.

Farquhar G.D., Lloyd J., Taylor J.A., Flanagan L.B., Syvertsen J.P., Hubick K.T., Wong S.C. & Ehleringer J.R. (1993) Vegetation effects on the isotope composition of oxygen in atmospheric CO_2. *Nature* **363,** 439–443.

Farquhar G.D., Cernusak L.A. & Barnes B. (2006) Heavy water fractionation during transpiration. *Plant Physiology* **143,** 11–18.

Farris F. & Strain B.R. (1978) The effects if water-stress on leaf $H_2{}^{18}O$ enrichment. *Radiation and Environmental Biophysics* **15,** 167–202.

Ferrio J.P., Florez-Sarasa I., Gessler A., Kodama N., Flexas J. & Ribas-Carbó M. (2012) The Péclet effect on leaf water enrichment correlates with leaf hydraulic conductance and mesophyll conductance for CO_2. *Plant, Cell and Environment* **35,** 611–625.

Fisher J.B., Malhi Y., Bonal D., Da Rocha H.R., *et al.* (2009) The land-atmosphere water flux in the tropics. *Global Change Biology* **15,** 2694–2714.

Flanagan L.B., Comstock J.P. & Ehleringer J.R. (1991) Comparison of modeled and observed environmental influences on the stable oxygen and hydrogen isotope composition of leaf water in *Phaseolus vulgaris* L. *Plant Physiology* **96,** 588–596.

Flanagan L.B., Phillips S.L., Ehleringer J.R., Lloyd J. & Farquhar G.D. (1994) Effects of changes in leaf water oxygen isotopic composition on discrimination against $C^{18}O^{16}O$ during photosynthesis. *Australian Journal of Plant Physiology* **21,** 221–234.

Franks P.J. (2006) higher rates of leaf gas exchange are associated with higher leaf hydrodynamic pressure gradients. *Plant, Cell & Environment* **29,** 584–592.

Gan K.S., Wong S.C., Yong J.W.H. & Farquhar G.D. (2003) Evaluation of models of leaf water 18O enrichment using measurements of spatial patterns of vein water, leaf water and dry matter in maize leaves. *Plant, Cell and Environment* **26,** 1479–1495.

Gat J.R. (1996) Oxygen and hydrogen isotopes in the hydrologic cycle. *Annual Review of Earth and Planetary Sciences* **24,** 225–262.

Griffis T.J., Lee X., Baker J.M., Sargent S.S.D. & King J.Y. (2005) Feasibility of quantifying ecosystem-atmosphere C18O16O exchange using laser spectroscopy and the flux gradient method. *Agricultural and Forest Meteorology* **135,** 44–60.

Griffis T.J., Lee X., Baker J.M., Billmar K., Schultz N., Erickson M., Zhang X., Fassbinder J., Xiao W. & Hu N. (2011) Oxygen isotope composition of evapotranspiration and its relation to C-4 photosynthetic discrimination. *Journal of Geophysical Research – Biogeosciences* **116,** G01035. doi:10.1029/2010JG001514.

Harwood K.G., Gillon J.S., Griffiths H. & Broadmeadow M.S.J. (1998) Diurnal variation of $\Delta^{13}CO_2$, $\Delta C^{18}O^{16}O$ and evaporative site enrichment of $\delta H_2{}^{18}O$ in *Piper aduncum* under field conditions in Trinidad. *Plant, Cell & Environment* **21,** 269–283.

Harwood K.G., Gillon J.S., Roberts A. & Griffiths H. (1999) Determinants of isotopic coupling of CO2 and water vapour within a *Quercus petraea* forest canopy. *Oecologia* **119,** 109–119.

Helliker B.R. & Ehleringer J.R. (2000) Establishing a grassland signature in veins: 18O in the leaf water of C3 and C4 grasses. *Proceedings of the National Academy of Sciences of the United States of America* **97,** 7894–7898.

Helliker B.R. & Noone D. (2010) Novel approaches for monitoring of water vapour isotope ratios: plants, lasers and satellites. In *Isoscapes: Understanding Movement, Pattern, and Process on Earth through Isotope Mapping* (eds J.B. West, G.J. Bowen, T.E. Dawson & K.P. Tu), pp. 71–88. Springer, New York.

Hendry M.J., Richman G. & Wassenaar L.I. (2011) Correction for methane interferences on δ^2H and $\delta^{18}O$ measurements in pore water using $H_2O_{(liquid)}$ – $H_2O_{(vapour)}$ equilibration laser spectroscopy. *Analytical Chemistry* **83,** 5789–5796.

Kahmen A., Simonin K., Tu K.P., Merchant A., Callister A., Siegwolf R., Dawson T.E. & Arndt S.K. (2008) Effects of environmental parameters, leaf physiological properties and leaf water relations on leaf water $\delta^{18}O$ enrichment in different *Eucalyptus* species. *Plant, Cell & Environment* **31,** 738–751.

Lee X., Sargent S., Smith R. & Tanner B. (2005) In situ measurement of the water vapour $^{18}O/^{16}O$ isotope ratio for atmospheric and ecological applications. *Journal of Atmospheric and Oceanic Technology* **22,** 555–565.

Majoube M. (1971) Fractionnement en oxygen-18 et en deuterium entre l'eau et sa vapeur. *Journal de Chimie et Physique* **58,** 1423–1436.

Merllivat L. (1978) Molecular diffusivities of $H_2{}^{18}O$ in gases. *Journal of Chemical Physics* **69,** 2864–2871.

Pataki D.E., Ehleringer J.R., Flanagan L.B., Yakir D., Bowling D.R., Still C.J., Buchmann N., Kaplan J.O. & Berry J.A. (2003) The application and interpretation of Keeling plots in terrestrial carbon cycle research. *Global Biogeochemical Cycles* **17,** 1022.

Schmidt M., Maseyk K., Lett C., Biron P., Richard P., Bariac T. & Seibt U. (2010) Concentration effects on laser-based $\delta^{18}O$ and δ^2H measurements and implications for the calibration of vapour measurements with liquid standards. *Rapid Communications in Mass Spectrometry* **24,** 3553–3561.

Seibt U., Wingate L., Berry J.A. & Lloyd J. (2006) Non-steady state effects in diurnal ^{18}O discrimination by *Picea sitchensis* branches in the field. *Plant, Cell & Environment* **29,** 928–939.

Tenhunen J.D., Valentini R., Kostner B., Zimmermann R. & Granier A. (1998) Variation in forest gas exchange at a landscape to continental scales. *Annales des Sciences Forestieres* **55,** 1–11.

Tyree M.T., Cruziat P., Benis M., LoGullo M.A. & Salleo S. (1981) The kinetics of rehydration of detached sunflower leaves from different initial water deficits. *Plant, Cell and Environment* **4,** 309–317.

Walker C.D. & Brunel J.-P. (1990) Examining evapotranspiration in a semi-arid region using stable isotopes of hydrogen and oxygen. *Journal of Hydrology* **118,** 55–75.

Walker C.D., Leaney F.W., Dighton J.C. & Allison G.B. (1989) The influence of transpiration on the equilibration of leaf water with atmospheric water vapor. *Plant, Cell & Environment* **12,** 221–234.

Wang L., Good S.P., Caylor K.K. & Cernusak L.A. (2011) Direct quantification of leaf transpiration isotopic composition. *Agricultural and Forest Meteorology* **154–155,** 127–135.

Wang X.-F. & Yakir D. (1995) Temporal and spatial variations in the oxygen-18 content of leaf water in different plant species. *Plant, Cell & Environment* **18,** 1377–1385.

Wang X.-F., Yakir D. & Avishai M. (1998) Non-climatic variations in the oxygen isotopic compositions of plants. *Global Change Biology* **4,** 835–849.

Welp L.R., Lee X., Kim K., Griffis T., Bilmark K. & Baker J. (2008) $\delta^{18}O$ of water vapour, evapotranspiration and the sites of leaf water evaporation in a soybean canopy. *Plant, Cell & Environment* **31,** 1214–1228.

White J.W.C. (1983) The climatic significance of D/H ratios in White Pine in the north-eastern United States. PhD thesis, Columbia University, New York.

Williams D.G., Cable W. & Hultine K. (2004) Evapotranspiration components determined by stable isotope, sap flow and eddy covariance techniques. *Agricultural and Forest Meteorology* **125,** 241–258.

Wingate L., Ogée J., Burlett R. & Bosc A. (2010) Strong seasonal disequilibrium measured between the oxygen isotope signals of leaf and soil CO_2 exchange. *Global Change Biology* **16,** 3048–3064.

Yakir D. & Sternberg L.S.L. (2000) The use of stable isotopes to study ecosystem gas exchange. *Oecologia* **123,** 297–311.

Yakir D., DeNiro M.J. & Rundel P.W. (1989) Isotopic inhomogeneity of leaf water: evidence and implications for the use of isotopic signals transduced by plants. *Geochimica et Cosmochimica Acta* **53,** 2769–2773.

Yakir D., DeNiro M.J. & Gat J.R. (1990) Natural deuterium and oxygen-18 enrichment in leaf water of cotton plants grown under wet and dry

conditions: evidence for water compartmentation and its dynamics. *Plant, Cell & Environment* **13,** 49–56.

Yakir D., Berry J.A., Giles L. & Osmond C.B. (1994) Isotopic heterogeneity of water in transpiring leaves: identification of the component that controls the $\delta^{18}O$ of atmospheric O_2 and CO_2. *Plant, Cell and Environment* **17,** 73–80.

Yepez E.A., Williams D.G., Scott R.L. & Lin G. (2003) Partitioning overstory and understory evapotranspiration in a semiarid savanna woodland from the isotopic composition of water vapour. *Agricultural and Forest Meteorology* **119,** 53–68.

Zwieniecki M.A., Brodribb T.J. & Holbrook N.M. (2007) Hydraulic design of leaves: insights from rehydration kinetics. *Plant, Cell & Environment* **30,** 910–921.

Received 14 May 2012; received in revised form 18 April 2013; accepted for publication 22 April 2013

SUPPORTING INFORMATION

Additional Supporting Information may be found in the online version of this article at the publisher's web-site:

Figure S1. Flow diagram for the MPH-1000 gas exchange system interfaced with the vaporization module and the infrared spectroscopy instrument.

Figure S2. Flow diagram for the two LI-6400 gas exchange systems interfaced with the vaporization module and the infrared spectroscopy instrument.